Optical probing of a silicon integrated circuit using electric-field-induced second-harmonic generation

Dong Xiao, Euan Ramsay, and Derryck T. Reid
Ultrafast Optics Group, School of Engineering and Physical Sciences, Heriot-Watt University, Edinburgh EH14 4AS, United Kingdom

Bernd Offenbeck and Norbert Weber
Fraunhofer-Institut für Integrierte Schaltungen, Optical Communications, Nordostpark 93, D-90411 Nürnberg, Germany

(Received 14 July 2005; accepted 17 January 2006; published online 17 March 2006)

By using the electric-field-induced second-harmonic generation effect, we have detected electrical signals present on a complementary metal-oxide-semiconductor (CMOS) integrated circuit in a noncontact geometry. Femtosecond pulses with a wavelength of 2.16 μm were incident on the device and the second harmonic at 1.08 μm exhibited a field-dependent behavior. The conversion efficiency from the fundamental to the second harmonic was estimated to be −103 dB. © *2006 American Institute of Physics*. [DOI: 10.1063/1.2180446]

In complementary metal-oxide-semiconductor (CMOS) integrated circuits direct electrical-contact probing of devices is often impractical and in modern flip-chip architectures is impossible because of the multiple wiring layers that obscure the semiconductor die. As a result, optical methods can be necessary to probe on-chip waveforms as part of the design cycle of a circuit. Existing techniques are limited, typically exploiting a weak effect in which carriers injected into a semiconductor junction induce an optically detectable change in the refractive index of the device.[1–4] We report an alternative approach using the electric-field-induced second-harmonic generation (EFISHG) technique[5,6] to probe voltages in a noncontact geometry. The technique uses mid-infrared femtosecond pulses to obtain observable EFISHG conversion efficiencies and this, combined with the instantaneous nature of EFISHG, means the method could enable THz-bandwidth probing of signals in CMOS circuits.

Optical probing of electric fields commonly exploits the electro-optic (EO) effect[7] in which a dc-field applied to a material with a nonzero $\chi^{(2)}$ susceptibility leads to an effective change in its $\chi^{(1)}$ susceptibility detectable as a change in its refractive indices. The EO effect has been used to sample the voltages in bulk semiconductors such as GaAs (Refs. 8 and 9) that possess a nonzero $\chi^{(2)}$ susceptibility and is also used in a probe geometry in which the evanescent coupling of an dc-field into a probe made from a noncentrosymmetric material such as $LiTaO_3$ results in a detectable polarization rotation.[10] Direct EO probing is not possible in the technologically important class of silicon devices because silicon belongs to the isotropic $m3m$ point group and therefore has no $\chi^{(2)}$ susceptibility. Probe-based EO sampling is also impractical in silicon integrated circuits because it requires close-coupling between the probe and the circuit but this is difficult because the semiconductor junctions are bounded on one side by metallisation layers and on the other by a thick silicon substrate. The EFISHG effect, although less well known, is analogous to the Pockels effect and can be observed in all materials. In EFISHG, an applied dc-field induces an effective $\chi^{(2)}$ susceptibility due to the action of the $\chi^{(3)}$ susceptibility.[5] EFISHG has been applied in the biological sciences,[11,12] in surface science,[12–14] and in organic chemistry to measure molecular hyperpolarizabilities,[15–17] but its potential for probing CMOS integrated circuits has remained undemonstrated, although EFISHG has been reported in several other custom silicon structures.[18–23] A feature of EFISHG in semiconductors is that, in order to minimize absorption of the generated second-harmonic (SH) light, the incident wavelength should be at least twice the band gap wavelength, hc/E_g, of the material and in silicon this implies a fundamental wavelength above 2.1 μm. Using sub-half-band-gap excitation also minimizes the creation of carriers in the device by linear or two-photon absorption and so the probing is less invasive and does not affect the result of the field measurement.[24]

In EFISHG, the $\chi^{(3)}(2\omega:0,\omega,\omega)$ susceptibility couples a dc-field, E_{dc} (in this context, one whose frequency is much smaller than typical optical carrier frequencies), to a coincident optical field, E_ω, to create an output field at the SH wavelength, $E_{2\omega}$, with an intensity $I_{2\omega} \propto |\chi^{(3)} E_{dc} E_\omega^2|^2$. The SH intensity depends quadratically on the dc field which itself varies in proportion to the voltage across the component under test. In silicon, the cubic symmetry means that the only nonzero elements of $\chi^{(3)}$ are[25] $\chi^{(3)}_{iiii}$ and $\chi^{(3)}_{iijj}$, so the strongest coupling between a linearly-polarized optical beam and the field in a planar silicon junction is obtained for p-polarized incident light (Fig. 1). Because the EFISHG signal is generated only in the forward direction we used a reflection geometry to collect SH light scattered from the ground electrode in a planar photodiode (Fig. 2).

EFISHG is extremely weak and so to generate observable amounts of SH light we used ultrafast pulses of durations around 160 fs. The pulses were generated by a periodically-poled lithium niobate optical parametric oscillator (OPO) that was synchronously pumped by a self-mode locked Ti:sapphire laser. We used the 2.16 μm idler pulses from the OPO as the fundamental light for the EFISHG experiment because silicon is transparent at this wavelength and the corresponding EFISHG wavelength of 1.08 μm, although near the band edge, is efficiently transmitted across the silicon substrate. We used a tightly-focused normal-incidence geometry that avoided the usual limitations of this approach by employing a near-infrared-corrected 0.42 NA

© 2006 American Institute of Physics
Downloaded 22 Jun 2006 to 137.195.28.161. Redistribution subject to AIP license or copyright, see http://apl.aip.org/apl/copyright.jsp

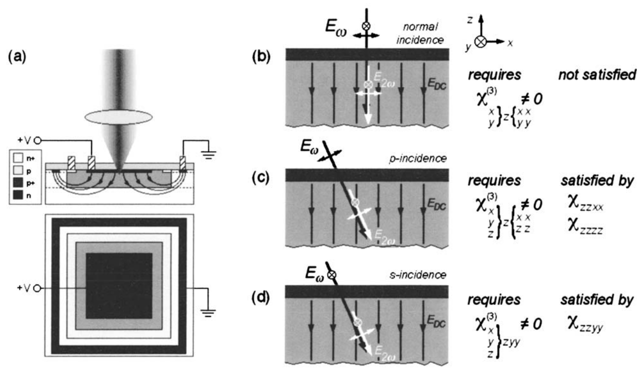

FIG. 1. (a) Incident light and electric field orientation relative to the photodiode junction plane. (b) Normal incidence requires tensor elements that are necessarily zero in silicon and yields no EFISHG. (c) *p*-polarized light can be coupled to the EFISHG field by both nonzero elements of the third-order susceptibility tensor. (d) *s*-polarized light is only coupled to the EFISHG field by the weaker off-diagonal tensor component.

microscope objective to ensure that a substantial amount of the fundamental light was incident at angles significantly less than 90° to the device plane and allowed us to access the nonzero components of the silicon $\chi^{(3)}$ susceptibility tensor. The 2.16 μm fundamental light was coupled into the device through a beamsplitter that was highly transmitting at 2.16 μm but highly reflecting at 1.08 μm and routed the SH light from the chip into a detection system comprising a Ge photodiode cooled to 77 K; a phase-sensitive amplifier and Ge and RG1000 optical filters situated before and after the sample, respectively, to discriminate against ambient light. After accounting for losses we estimated an average (peak) power at the device of around 20 mW (1.2 kW), corresponding to a peak intensity of 5.8 GW cm^{-1}.

We carried out EFISHG probing near the edge of a 500 μm $\times$ 500 μm shallow photodiode in which a planar p^+-n junction was formed between a 200 nm thick p^+ electrode and a 2 μm thick n electrode and was reverse biased from 0 to 1.8 V. The reverse bias circuit was a dc supply in series with the photodiode and an external resistor. Although an EFISHG signal was detectable across the whole area of the device, the strongest signal was observed at the edge because here the dc field in the sample can be nearly parallel

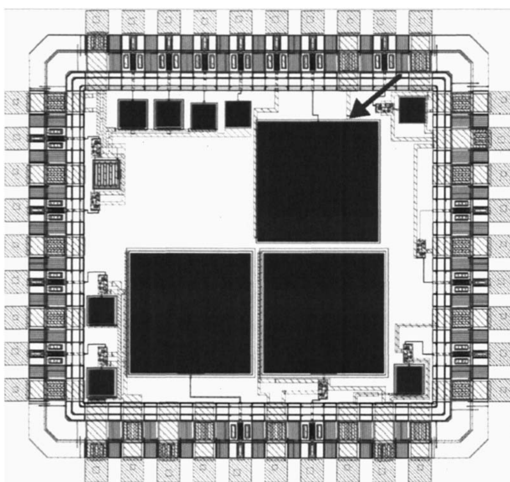

FIG. 2. CMOS integrated circuit containing planar photodiode structures in shallow and deep diffusion geometries and EFISHG probing location (arrow).

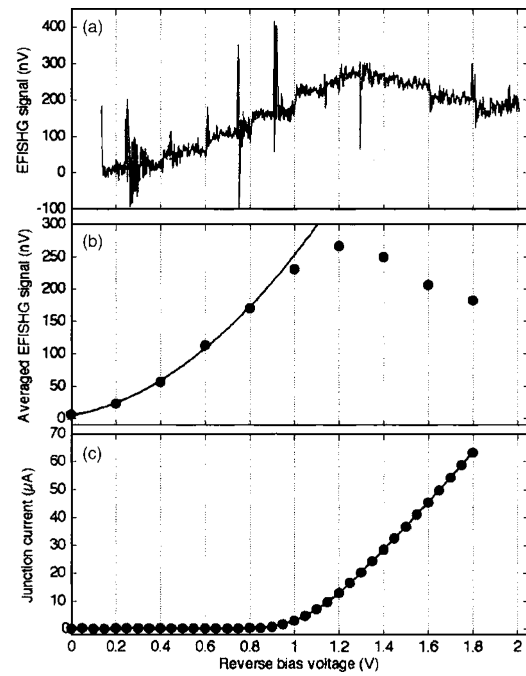

FIG. 3. (a) Unprocessed EFISHG signal for bias voltages from 0 to 1.8 V. The leftmost box shows data obtained at 0 V bias and subsequent boxes correspond, left to right, to constant bias voltages incremented in 0.2 V steps. A background signal obtained with the laser blocked has been removed. (b) Averaged EFISHG signals shown with a quadratic fit. (c) Current-voltage characteristic measured under reverse bias conditions.

to the optical field and the EFISHG signal is generated by the strong $\chi^{(3)}_{iiii}$ components of the susceptibility tensor. The reverse-bias voltage was increased in steps of 0.2 V and at each value the EFISHG signal was recorded for 100 s [Fig. 3(a)]. Using lock-in detection, the maximum field-dependent EFISHG signal change was ~500 nV with a signal to noise ratio of 8:1 and we estimated the absolute average power of the SH light to be 1 pW based on the signal level observed with a near-infrared photomultiplier tube and the quoted responsivity of this detector. This power level implies an optical conversion efficiency of -103 dB and compares well with a value estimated by treating the EFISHG process as a conventional SH interaction with a susceptibility of $\chi^{(2)}_{\mathrm{eff}} = \chi^{(3)} E_{\mathrm{DC}}$. For a p^+-n junction in which the acceptor density, N_a, is much greater than the donor concentration, N_d, theory gives the transition region width as $W = \sqrt{2\varepsilon V / e N_d}$, where ε is the static dielectric constant of silicon and V is the applied voltage. The doping concentration of our device was unavailable to us but typically $N_d = 10^{16}$ cm^{-3}, implying a transition region width of 360 nm. Taking this value, a bias of 1 V creates a field of $E_{\mathrm{dc}} = 2.8$ V μm^{-1} spanning the whole area of the photodiode structure. The third-order susceptibility can be estimated as $\chi^{(3)} \approx 1.4 \times 10^{-19}$ pm^2 V^{-2}, based on a published value of the nonlinear refractive index for silicon[26] of $n_2 = 4.5 \times 10^{-14}$ cm^2 W^{-1}. The coherence length in silicon for SHG from 2.16 μm to 1.08 μm is 5 μm and so, by assuming conversion occurs over one coherence length and is described by the plane-wave solution to the nonlinear coupled-wave equations, one arrives at an estimate for the conversion efficiency of -104 dB.

The results in Fig. 3(b) show the average background-removed EFISHG signal recorded at each bias voltage along with a quadratic fitted to the 5 data points obtained at reverse bias voltages below 1 V. The quadratic intercepts the voltage

Downloaded 22 Jun 2006 to 137.195.28.161. Redistribution subject to AIP license or copyright, see http://apl.aip.org/apl/copyright.jsp

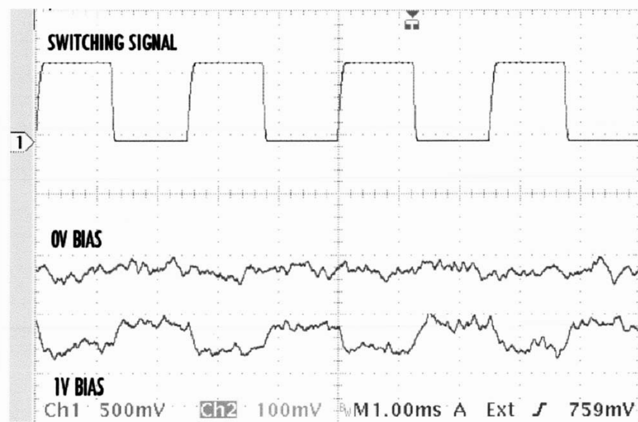

FIG. 4. Composite oscilloscope image showing the EFISHG signal obtained in real-time using an infrared-sensitive photomultiplier tube. The top signal shows the switching waveform used to modulate the applied dc bias. The lower signals are dynamic averages over 512 traces and show the EFISHG signal for reverse biases of 0 V and 0.5 V.

axis at a small value of forward bias ($V_{bias} \sim -0.15$ V) and represents an estimate of the unction contact potential. This behavior is typical for EFISHG measurements across silicon junctions and is consistent with results reported elsewhere.[6,21] As expected, the EFISHG signal increased quadratically with increasing reverse bias up to a maximum but then began to decrease as the bias continued to rise. Such behavior can be interpreted as follows. As a reverse bias is applied, the field across the junction rises and so the EFISHG signal increases. Once the electric field in the junction exceeds the Zener breakdown field the junction becomes conducting and the voltage dropped across the external resistor increases while the voltage across the junction falls, reducing the internal junction field and resulting in a lower EFISHG signal for reverse bias voltages above 1 V. This interpretation is supported by a current-voltage measurement of the junction recorded under reverse bias [Fig. 3(c)] which shows the onset of Zener breakdown at a bias voltage very close to the maximum of the EFISHG signal.

Because EFISHG is instantaneous and is naturally associated with ultrafast stimulation it could enable high-bandwidth subsurface optical probing in CMOS silicon devices in a similar way to that already demonstrated for silicon coplanar transmission lines.[27] Two possible approaches exist for using EFISHG for high speed probing, namely direct broad-bandwidth detection of EFISHG signal or synchronous electrical-optical stimulation in which a time-delayed optical pulse at the fundamental wavelength samples the field in a circuit in synchronism with an electrical waveform pattern written to the device. As a proof-of-principle of the former approach we excited the photodiode by setting the reverse bias voltage to either 0 V or 0.5 V then periodically switching the bias on and off using 400 Hz a square wave (Fig. 4). For high speed detection we used a near-infrared photomultiplier tube (Hamamatsu H9170-75) and the results indicate that an EFISHG signal can be detected in real time. The few ns risetime of the photomultiplier tube limits the direct detection method to sub-GHz frequencies but for many applications this may be sufficient.

Although we have demonstrated that EFISHG can be used to sample the field in CMOS devices there is further work needed before the technique can be a practical tool for probing integrated circuits. In particular, the extension to through-substrate probing will allow EFISHG to be realised in flip-chip integrated circuits. We expect that the EFISHG signal levels could be improved substantially by adopting a subsurface solid-immersion imaging geometry[28,29] in which a silicon solid-immersion lens is placed in contact with the device substrate and leads to a large increase of the solid-angle inside the substrate. The higher NA achievable in this way gives superior optical resolution and should allow more efficient conversion due to the larger component of the incident polarization lying normal to the device plane.

The authors are grateful to the UK EPSRC for financial support under grant reference No. GR/S62819/01 and to Hamamatsu for the loan of the H9170-75 photomultiplier tube.

[1] R. K. Thalhammer and G. K. M. Wachutka, IEEE Trans. Comput.-Aided Des. **23**, 60 (2004).
[2] H. K. Heinrich, D. M. Bloom, and B. R. Hemmenway, Appl. Phys. Lett. **48**, 1066 (1986).
[3] M. Goldstein, G. Sölkner, and E. Gornik, Rev. Sci. Instrum. **64**, 3009 (1993).
[4] M. Goldstein, G. Sölkner, and E. Gornik, Microelectron. Eng. **24**, 431 (1994).
[5] R. W. Terhune, P. D. Maker, and C. M. Savage, Phys. Rev. Lett. **8**, 404 (1962).
[6] C. H. Lee, R. K. Chang, and N. Bloembergen, Phys. Rev. Lett. **18**, 167 (1967).
[7] T. Nagatsuma, IEICE Trans. Electron. **E76c**, 55 (1993).
[8] B. H. Kolner and D. M. Bloom, Electron. Lett. **20**, 818 (1984).
[9] C. J. Madden, R. A. Marsland, M. J. W. Rodwell, D. M. Bloom, and Y. C. Pao, Appl. Phys. Lett. **54**, 1019 (1989).
[10] J. A. Valdmanis, Electron. Lett. **23**, 1308 (1987).
[11] P. J. Campagnola, M. D. Wei, A. Lewis, and L. M. Loew, Biophys. J. **77**, 3341 (1999).
[12] V. I. Gavrilenko, Phys. Status Solidi A **188**, 1267 (2001).
[13] P. Godefroy, W. de Jong, C. W. van Hasselt, M. A. C. Devillers, and T. Rasing, Appl. Phys. Lett. **68**, 1981 (1996).
[14] I. Thom and M. Buck, Surf. Sci. **581**, 33 (2005).
[15] K. Clays and A. Persoons, Phys. Rev. Lett. **66**, 2980 (1991).
[16] L. T. Cheng, W. Tam, S. H. Stevenson, G. R. Meredith, G. Rikken, and S. R. Marder, J. Phys. Chem. **95**, 10631 (1991).
[17] L. T. Cheng, W. Tam, S. R. Marder, A. E. Stiegman, G. Rikken, and C. W. Spangler, J. Phys. Chem. **95**, 10643 (1991).
[18] O. A. Aksipetrov, A. A. Fedyanin, V. N. Golovkina, and T. V. Murzina, Opt. Lett. **19**, 1450 (1994).
[19] O. A. Aksipetrov, A. A. Fedyanin, E. D. Mishina, A. N. Rubtsov, C. W. van Hasselt, M. A. C. Devillers, and T. Rasing, Phys. Rev. B **54**, 1825 (1996).
[20] G. Lupke, C. Meyer, C. Ohlhoff, H. Kurz, S. Lehmann, and G. Marowsky, Opt. Lett. **20**, 1997 (1995).
[21] J. I. Dadap, J. Shan, A. S. Weling, J. A. Misewich, and T. F. Heinz, Appl. Phys. B **68**, 333 (1999).
[22] T. V. Dolgova, A. A. Fedyanin, and O. A. Aktsipetrov, Phys. Rev. B **68**, 0733071–4 (2003).
[23] R. Pasternak, A. Chatterjee, Y. V. Shirokaya, B. K. Choi, Z. Marka, J. K. Miller, R. G. Albridge, S. N. Rashkeev, S. T. Pantelides, R. D. Schrimpf, D. M. Fleetwood, and N. H. Tolk, IEEE Trans. Nucl. Sci. **50**, 1929 (2003).
[24] K. A. Peterson and D. J. Kane, Opt. Lett. **26**, 438 (2001).
[25] W. K. Burns and N. Bloembergen, Phys. Rev. B **4**, 3437 (1971).
[26] M. Dinu, F. Quochi, and H. Garcia, Appl. Phys. Lett. **82**, 2954 (2003).
[27] A. Nahata, T. F. Heinz, and J. A. Misewich, Appl. Phys. Lett. **69**, 746 (1996).
[28] S. B. Ippolito, B. B. Goldberg, and M. S. Ünlü, Appl. Phys. Lett. **78**, 4071 (2001).
[29] E. Ramsay, N. Pleynet, D. Xiao, R. J. Warburton, and D. T. Reid, Opt. Lett. **30**, 26 (2005).

Downloaded 22 Jun 2006 to 137.195.28.161. Redistribution subject to AIP license or copyright, see http://apl.aip.org/apl/copyright.jsp